AN ANALYSIS OF THE AIR-JET YARN-TEXTURING PROCESS PART IV: FLUID FORCES ACTING ON THE FILAMENTS AND THE EFFECTS OF FILAMENT CROSS-SECTIONAL AREA AND SHAPE

M. ACAR, R. K. TURTON, and G. R.WRAY
Loughborough University, UK

ABSTRACT

Fluid (drag) forces acting on filaments in an air-flow are theoretically analysed, and equations to calculate them are derived. Drag forces acting on filaments are shown to vary with the filament cross-section, the position of the filaments across the nozzle, and the local air velocity. Since finer filaments have a smaller inertial resistance to fluid forces and have lower stiffness, yarns with finer filaments are shown to be more suitable for air-jet texturing. Theoretical modelling of a lament as it emerges from the nozzle shows that, for filaments with identical linear densities, those with cross sections having reduced bending and torsional stiffness, such as elhpt1c cross-sections, may be more suitable for air-jet texturing.

INTRODUCTION

In the air-jet texturing process, the forces acting on the filaments are the forces due to primary flow, F_P, the forces due to secondary flow, F_s, and the frictional forces, F_f, as shown in Fig. 1. In particular, frictional forces play an important role m the texturing process, as will later be shown in Part V of this series[1] In the following analysis of the fluid forces, only primary-flow effects will be considered, but it should be noted that the approach used here could also be applied to the secondary flow.

FLUID FORCES ACTING ON THE FILAMENTS

The fluid forces acting on the filaments are very complex, not only because of the complex nature of the air-flow itself, but also because of the extremely rapid movement of the filaments in the nozzle and interactions between the air-flow and the filaments. In addition, frictional forces between the filaments themselves and between them and other components, such as the nozzle, yarn guides, and wetting unit (see Fig. 1), will complicate the analysis of fluid forces acting on the filaments.
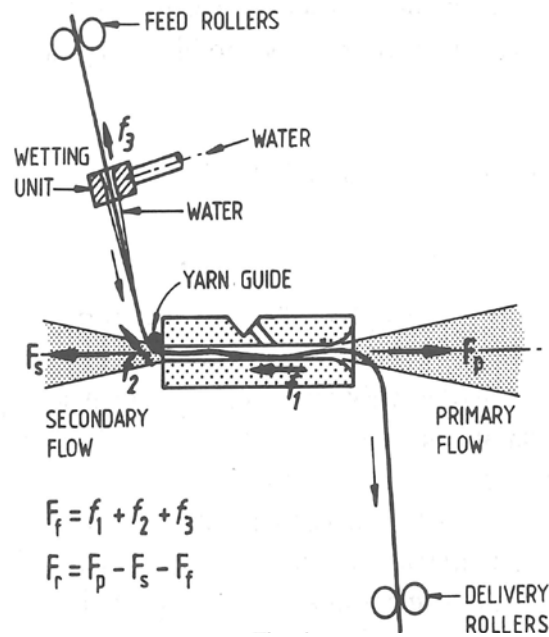
Fig. 1. Schematic diagram of the feed and delivery zones, showing the
frictional forces acting on the filaments

In order to simplify the analysis, a short incremental section of a single filament,
subject to the air-flow in the texturing nozzle as shown in Fig. 2, is considered.
It is assumed firstly that this filament increment is rigid (in order to simplify
analysis by applying the laws of mechanics) and secondly that its motion is two-
dimensional, i.e., parallel to the xy-plane.

$$V_n = (u - u_G) \sin\phi + (v - v_G)\cos\phi + r\dot\phi$$

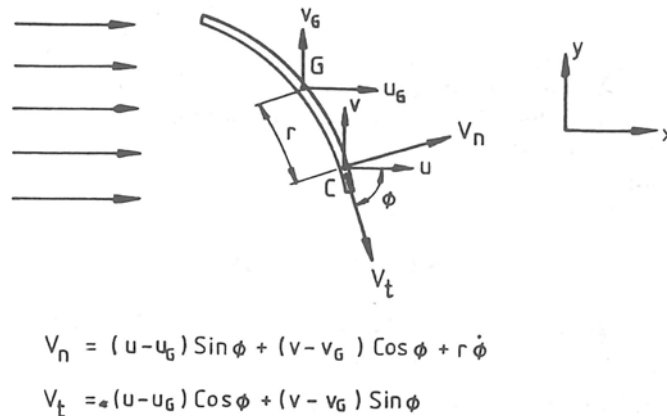$$V_t = (u - u_G)\cos\phi + (v - v_G)\sin\phi$$

Fig. 2. Incremental textile fibre in an air-flow

The resultant forces and moments acting on the fibre are generated by the
relative velocity between the fibre and the surrounding air-flow. The velocity
components of its centre of mass, G, are u_g and v_g; V_n and V_t; are the normal and
tangential velocity components relative to the air-flow, respectively, of an
arbitrary point on the fibre a distance r from G; u and v are the velocity
components of the air-flow adjacent to the same point on the fibre. Hence, with
reference to Fig. 2, V_n and V_t; can be expressed as follows:

$$V_n = (u - u_g) \sin \phi + (v - v_g) \cos \phi + r\dot{\phi} \tag{1}$$

and

$$V_t = (u - u_g) \cos \phi - (v - v_g) \sin \phi \ . \tag{2}$$

(It will be noted that V_n and V_t vary from point to point along the fibre increment because of the spatial variations of u and v, because of the changing values of r, and because of the fibre motion.)

Fluid forces acting on the filaments can be expressed in terms of the pressure- and frictional-drag forces. The pressure drag, D_P, is caused by the pressure difference between the two sides of the filament in a cross flow (V_n). The drag on an element can be expressed in terms of a drag coefficient for a length d*l*as:

$$dD_p = \frac{1}{2} (C_p \rho d_f V_n^2 dl), \tag{3}$$

where $\quad$ C_p is the drag coefficient for pressure drag;

ρ is the fluid density; and

d_f *is* the fibre diameter.

On integrating, we have:

$$D_p = \rho \frac{d_f}{2} \int_{-L/2}^{L/2} C_p V_n^2 dl \ , \tag{4}$$

where L is the length of the fibre exposed to the flow.

As can be seen from Equation (4), the pressure drag is a function of the projected area of the fibre:

$$A_p = d_f L \ .$$

The frictional drag, D_f, is caused by the frictional forces between the fibre and tangential air-flow (v_t), which can be formulated as for the pressure drag, and:

$$D_f = \rho \frac{d_f}{2} \int_{-L/2}^{L/2} C_f V_t^2 dl \ , \tag{5}$$

where C_f is the drag coefficient for the frictional drag.

Frictional drag, as expressed in Equation (5), is a function of the fibre-surface area:

$$A_s = \pi d_f L \ .$$

Hence the fluid forces in the x and y directions are:

$$D_x = D_p \sin \phi + D_f \cos \phi \ . \tag{6}$$

and

$$D_y = D_p \cos \phi + D_f \sin \phi \ . \tag{7}$$

As Equations (6) and (7) indicate, the fluid forces in the x and y directions are functions of the normal and tangential components of the flow velocity, V_n and V_f the angle of attack, Φ, of the air-flow, and the projected and surface areas, A_p and A_s of the fibre within the flow.

The resultant force, F_r, acting on an individual filament in an air-jet texturing nozzle is determined by the fluid forces, i.e., F_P and F_s, acting on the segment of the filament within the nozzle and by the total frictional force, F_f, due to contacts it makes with: (i) the nozzle internal surfaces, f_1 (ii) the yarn guides, f_2; and (iii) the wetting unit, f_3 (see Fig. 1). In addition to these frictional forces, there also occurs a further frictional force due to the longitudinal movement of the filaments relative to each other; such frictional aspects will be investigated in Part V of this series of papers[1] Since the primary flow is stronger than the secondary flow, because of the greater momentum transferred to it from the incoming jets owing to the orientation of their inlet bores, the resultant fluid force acting on the filaments is in the direction of the primary flow, i.e., $F_p > F_f$. The resultant force, F_r, acting on a filament is therefore:

$$F_r = F_p - F_s - F_f \, , \tag{8}$$

as shown in Fig. 1.

FACTORS AFFECTING FLUID FORCES

Drag Force

The drag force acting on a filament under any given flow conditions is a function of the local air velocity and of the filament surface and the projected areas exposed to the flow. The air velocity is mainly determined by the air-supply pressure, whereas the velocity gradient is determined by the design of the nozzle as discussed in Part II of this series of Papers[2]. The surface and projected areas exposed to flow are determined by the position of the filament across the nozzle, its cross-section, and its orientation.

Filament Position

The surface area of a filament exposed to flow is determined by the length of the filament in the air stream, whereas the instantaneous projected area depends on the position of the filament in the nozzle. Although the surface area of a filament subject to the flow m the nozzle does not vary significantly with its position, its projected area doe vary considerably. A filament within the upper part of the nozzle has a greater projected area than a filament within the lower part (Fig. 3) and is therefore subject to higher fluid forces; the different fluid forces acting on the filaments at different positions in the nozzle at any instant cause them to travel at different speeds and hence to be displaced longitudinally relative to each other.

Filament Cross-section

A circular filament of larger diameter will give rise to greater drag forces owing to its greater projected area and surface area, since F, is proportional to dr. On the other hand, its inertial resistance to the fluid forces is expressed in terms of the momentum flux required to move these filaments, which can be expressed as follows:

$$\dot{m}_f V_f = \left(\frac{\pi}{4} \, d_f^2 \rho_f V_f \right) V_f \, ,$$

where m_f is the mass-flow rate of the filaments; ρ_f is the filament density; and V_f is the filament velocity. This is a function of the filament cross-sectional area, i.e., it is proportional to d_f^2. An increase in filament diameter thus causes the fluid forces to increase proportionally with the filament diameter, but the force required to overcome the inertia and to move this thicker filament will increase with the square of the filament diameter. Consequently, a decrease in the filament diameter will allow it to be blown out at a higher speed. A further factor to be taken into account is that filaments with smaller diameters have a lower bending stiffness, which will facilitate the loop-formation process. For yarns of the same linear density, finer-filament yarns will possess more filaments, which thus increase the probability of inter-filament entanglements. All these factors lead to the conclusion that supply yarns that are composed of finer filaments should texture more satisfactorily than coarser-filament yarns.
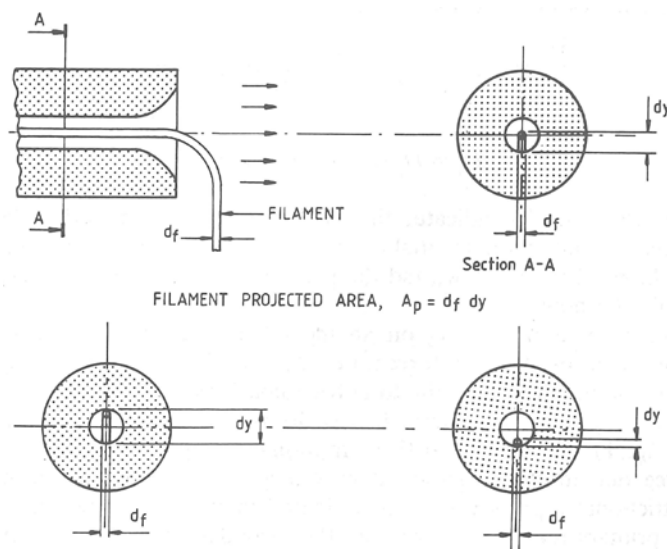

Fig. 3. Schematic illustration of the variation of the filament projected area with its position in the nozzle

EFFECTS OF THE FILAMENT CROSS-SECTION

Introduction

The area-dependent mechanical properties of the filaments vary with the shape of their cross-sections. These will also have an effect on the forces required to deflect the filaments at right angles as they emerge from the nozzle. The fluid forces acting on the filaments will also vary owing to the different surface and projected areas arising from non-circular cross-sectional shapes. These factors may have an effect on the loop- formation process.

In order to analyse the effect of the shape of the filament cross-section on loop formation, filaments with various cross-sectional shapes but with the same cross-sectional areas (i.e., identical linear densities) may be considered; regardless of the cross-sectional shapes, the inertia that has to be overcome in order to move the filaments then remains the same.
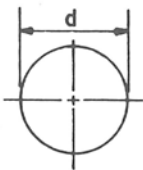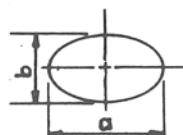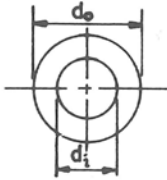
The analysis presented here is confined to a comparison of circular filaments with hypothetical filaments of elliptical and hollow-circular (annular) cross-

sections. Examples of other cross-sections, such as trilobal, octalobal, etc. (which are admittedly more representative of commercially available filament types), could also have been considered; however, the above-mentioned three types are sufficient to illustrate the principal effects. Some area properties of the three assumed cross-sectional shapes are given in Table I.

Effects on the Drag Forces

Since the total drag force acting on the filaments, as shown in Section 2, is dependent on the surface and projected areas of the filaments in the flow, varying the shapes of the filament cross-sections will affect the drag force.

Table I
Area Properties of Circular, Elliptic, and Hollow-circular Cross-sections

Cross-sectional Shape	Second Moment of Area, I, about a Diameter	Polar Second Moment of Area, J	Periphery, P
Circular	$\pi d^4/64$	$\pi d^4/32$	πd
Elliptical	$I_x = \pi ab^3/4$ $I_y = \pi a^3 b/4$	$\pi ab(a^2 + b^2)/4$	$\pi\left\{\dfrac{a^2 + b^2}{2}\right\}^{1/2}$ (approx.)
Hollow-circular	$\pi(d_0^4 - d_i^4)/64$	$\pi(d_0^4 - d_i^4)/32$	πd_0

When an elliptic filament bends about its major diameter under a bending moment, its projected area is ($n^{1/2}$) times, and its surface area is $\{(n^2 + 1)/2n\}^{1/2}$ times as large as that of a circular filament of equal cross-sectional area, where n is the ratio of the major to the minor diameter of the ellipse (see Table II). Hence the drag force acting on an elliptic filament will be larger than that acting on a circular filament of equal fineness. The higher the ratio of major to minor diameter, the greater becomes the drag forces. A similar argument is valid for a hollow-cross-section filament (Table II), which will also generate a greater drag force.

Table II
Comparison of Second Moment of Area and Surface and Projected Areas of Circular, Elliptic, and Hollow-circular Cross-sectional Filaments*.

Cross-sectional Shape	Second Moment of Area, about a Diameter, I	Polar Second Moment of Area, J	Surface Area, A_s	Projected Area, A_p
Circular	1	1	1	1
Elliptical	$1/n$ (about major diameter)	$2n/(n^2+1)$	$[9n^2+1)/2n]^{1/2}$ (approx.)	$n^{1/2}$
Hollow-circular	$(n^2+1)/(n^2-1)$	$(n^2+1)/(n^2-1)$	$n/(n^2-1)^{1/2}$	$n/(n^2-1)^{1/2}$

* n = Ratio of major to minor diameter for elliptical cross-sections and ratio of outer to inner diameter for hollow-circular (annular) cross-sections.

Effects on the Bending and Torsional Properties

During the texturing process, the filaments emerging from the nozzle make a right-angled turn relative to the nozzle exit. Fig. 4 represents a single filament emerging from the nozzle during the texturing process on the assumption that it forms a circular arc while making a right-angled turn. The leading end (A) of the filament is instantaneously fixed in the textured yarn, and the fluid forces causing the filaments to be blown out of the nozzle are assumed to be acting at the trailing end (B). This filament may also be subject to a twisting action (as was consistently observed experimentally as a result of the swirling effect of the flow), and it is therefore subject to both a bending moment and a torque. These will cause instantaneous vertical and horizontal deflexions of point B as well as a torsional deflexion of the filament.
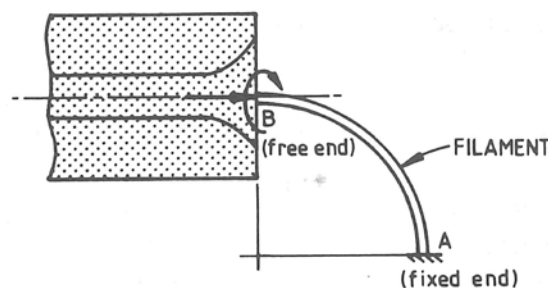

Fig. 4. A section of a filament making a right-angled turn on emerging from the nozzle

It is known that bending and torsional stiffnesses are directly proportional to the second moment of area about a diameter and to the polar second moment of area, respectively; the smaller these second moments of area, the smaller are the forces and torques required to bend and twist the filament, respectively.

Table II shows that both the second moments of area of an ellipse are smaller than those of a circle of equal cross-sectional area; it may be concluded that smaller forces and torques are required to deflect a filament that has an elliptic cross-section and that the higher the ratio of the major to minor diameter ($n = a/b$), the smaller become the force and torque required to deflect that filament. In addition to bending and torsion, this filament may also be subject to buckling. Since the critical buckling load is proportional to the smaller principal second moment of area of a cross-section, buckling of an elliptic filament occurs about

its major axis, and the critical buckling load for an elliptical cross-section is smaller than that for a circular cross-section.

Table II also shows that the second moment of area and the second polar moment of area of a hollow-circular fibre are larger than those for a solid circular fibre of equal fineness. This leads to the conclusion that larger forces and torques are required to deflect the hollow fibre than are required for the solid circular fibre.

DISCUSSION AND CONCLUSIONS

The model considered in the previous section assumes that the filaments make a circular arc and that the fluid forces are concentrated at the trailing end of the filament. This is usually not the case, the real situation being much more complex. Filaments, although they make a right-angled turn, may assume shapes other than circular arcs, and these would affect the bending and torsional behaviour of the filaments as well as the fluid forces acting on them. Nevertheless, all the filaments make an eventual right-angled turn with respect to the nozzle axis, and they are subject to fluid forces that make them bend, twist, and buckle. The following general conclusions derived from the model discussed in the previous section are essentially valid for any texturing conditions:

(i) circular filaments with finer linear density are more suitable for air-jet texturing because their bending and torsional stiffnesses and their inertial resistance are smaller; smaller drag forces are required to blow them out of the nozzle, and they bend more easily during loop formation;

(ii) non-circular and hollow filaments have a larger (surface area/volume) ratio and are thus subjected to greater frictional-drag forces in relation to their inertia;

(iii)) a similar situation occurs with pressure-drag forces because the projected areas are also greater, in view of the fact that non-circular filaments have a preferred bending direction about a major axis; and

(iv) hollow filaments have a greater surface area and projected area but are also stiffer in both the torsional and bending modes; in this case, it is not clear where the advantages lie, but one advantage may be increased bulk due to the hollow structure of the filaments.

It is suggested that the use of supply yarns composed of non-circular (e.g., trilobal) and hollow filaments could be worthy of further experimental investigation, since, for some applications, they may have technological advantages over the air-jet texturing of yarns with conventional circular-shaped filaments.

REFERENCES

1. M. Acar, R. K. Turton, and G. R. Wray. *J. Text. Inst.,* to be published (Part V of this series of papers).

2. M. Acar, R. K. Turton, and G. R. Wray. *J. Text. Inst.,* 1986, 77, 28.